# Hexacarbonyldiplatinum(I). Synthesis, Spectroscopy, and Density Functional Calculation of the First Homoleptic, Dinuclear Platinum(I) Carbonyl Cation, [{Pt(CO)3}2]2+, Formed in Con...

**ARTICLE** *in* JOURNAL OF THE AMERICAN CHEMICAL SOCIETY · JULY 2000

Impact Factor: 12.11 · DOI: 10.1021/ja000716u

# Hexacarbonyldiplatinum(I). Synthesis, Spectroscopy, and Density Functional Calculation of the First Homoleptic, Dinuclear Platinum(I) Carbonyl Cation, $[\{Pt(CO)_3\}_2]^{2+}$, Formed in Concentrated Sulfuric Acid

**Qiang Xu,*,† Brian T. Heaton,‡ Chacko Jacob,‡ Koichi Mogi,§ Yuichi Ichihashi,† Yoshie Souma,† Kan Kanamori,|| and Taro Eguchi⊥**

*Contribution from Osaka National Research Institute, AIST, MITI, Midorigaoka, Ikeda, Osaka 563-8577, Japan, Department of Chemistry, The University of Liverpool, Crown Street, Liverpool L69 7ZD, UK, Department of Molecular and Material Sciences, Graduate School of Engineering Sciences, Kyushu University, Kasuga, Fukuoka 816-8580, Japan, Department of Chemistry, Toyama University, 3190, Gofuku, Toyama 930-8555, Japan, and Department of Chemistry, Graduate School of Science, Osaka University, Toyonaka, Osaka 560-0043, Japan*

*Received February 28, 2000*

**Abstract:** The dissolution of $PtO_2$ in concentrated $H_2SO_4$ under an atmosphere of CO results in the formation of hexacarbonyldiplatinum(I), $[\{Pt(CO)_3\}_2]^{2+}$ (**1**), the first homoleptic, dinuclear, cationic platinum carbonyl complex, of which a prolonged evacuation leads to reversible disproportionation to give *cis*-$[Pt(CO)_2]^{2+}{}_{(solv)}$ (**2**) and Pt(0). **1** has been completely characterized by NMR ($^{13}C$ and $^{195}Pt$), IR, Raman, and EXAFS spectroscopy. The structure of **1** is rigid on the NMR time scale at room temperature. NMR: $\delta(^{13}C^A)$ 166.3, $\delta(^{13}C^B)$ 158.7, $\delta(^{195}Pt)$ −211.0 ppm; $^1J(Pt-C^A) = 1281.5$ Hz, $^1J(Pt-C^B) = 1595.7$ Hz, $^1J(Pt-Pt') = 550.9$ Hz. The strongly polarized, sharp Raman band at 165 $cm^{-1}$ ($\rho$ = ca. 0.25) indicates the presence of a direct Pt−Pt bond. The IR and Raman spectra in the CO stretching region are entirely consistent with the presence of only terminal CO's on a nonbridged Pt−Pt bond with $D_{2d}$ symmetry. $\nu(CO)_{IR}$: 2174 ($E$), 2187 ($B_2$), and 2218 $cm^{-1}$ ($B_2$); $\nu(CO)_{Raman}$: 2173 ($E$), 2194 ($B_2$), 2219 ($B_2$), 2209 ($A_1$) and 2233 $cm^{-1}$ ($A_1$). EXAFS measurements show that the Pt−Pt bond is 2.718 Å and the mean length of the Pt−C bonds is 1.960 Å. The geometric optimization for **1** by a density functional calculation at the B3LYP level of theory predicts that the dinuclear cation contains two essentially planar tricarbonyl platinum(I) units that are linked via a Pt−Pt bond about which they are twisted by exactly 90.0° with respect to each other.

## I. Introduction

Platinum carbonyl compounds have the longest history and have assumed a very important position in metal carbonyl chemistry.[1] The platinum(II) carbonyl chlorides, $Pt(CO)_2Cl_2$, $Pt(CO)Cl_2$, and $Pt_2(CO)_3Cl_4$, reported by Schützenberger in 1870,[2] were the first metal carbonyl derivatives to be synthesized. Homoleptic platinum carbonyl complexes have also been isolated and observed in solution and matrices. Compounds of platinum(0) containing only carbon monoxide, such as $Pt(CO)_n$ ($n = 1-4$), remain accessible only by matrix isolation methods.[3] In the 1970s, homoleptic, anionic platinum carbonyl clusters, e.g. $[Pt_3(CO)_6]_n^{2-}$ ($n = \sim 10, 6, 5, 4, 3, 2, 1$) and $[Pt_{19}(CO)_{12}(\mu_2\text{-}CO)_{10}]^{4-}$, in which the Pt atoms are bridged by CO ligands, were reported.[4] They are usually prepared by the reductive carbonylation of platinum halides in basic media. Recently, infrared spectroelectrochemistry has been utilized to explore the vibrational properties of the anionic, high-nuclearity platinum carbonyl clusters $[Pt_{24}(CO)_{30}]^n$, $[Pt_{26}(CO)_{32}]^n$, and $[Pt_{38}(CO)_{44}]^n$ ($n = 0$ to 10−) as a function of the charge $n$ in several solvents.[5] The homoleptic platinum(II) carbonyl cation, $[Pt(CO)_4]^{2+}$, has recently been reported.[6]

In the past 10 years, there has been a rapid development in the preparation and characterization of new homoleptic metal carbonyl cations, including $[Pt(CO)_4]^{2+}$.[7] This new class of metal carbonyl complexes includes metals from groups 6 through 12

* To whom correspondence should be addressed. E-mail: xu@onri.go.jp. Phone: +81-727-51-9652.

† Osaka National Research Institute.

‡ The University of Liverpool.

§ Kyushu University.

|| Toyama University.

⊥ Osaka University.

(1) (a) Tripathi, S. C.; Srivastava, S. C.; Mani, R. P.; Shrimal, A. K. *Inorg. Chim. Acta* **1976**, *17*, 257. (b) Roundhill, D. M. In *Comprehensive Coordination Chemistry*; Pergamon Press: Oxford, England, 1987; Vol. 5, p 377.

(2) (a) Schützenberger, P. *C. R. Hebd. Seances Acad. Sci.* **1870**, *70*, 1134. (b) Schützenberger, P. *C. R. Hebd. Seances Acad. Sci.* **1870**, *70*, 1287. (c) Schützenberger, P. *Bull. Chim. Fr.* **1870**, *14*, 97.

(3) Kündig, E. P.; McIntosh, D.; Moskovits, M.; Ozin, G. A. *J. Am. Chem. Soc.* **1973**, *95*, 7234.

(4) (a) Calabrese, J. C.; Dahl, L. F.; Chini, P.; Longoni, G.; Martinengo, S. *J. Am. Chem. Soc.* **1974**, *96*, 2614. (b) Longoni, G.; Chini, P. *J. Am. Chem. Soc.* **1976**, *98*, 7225. (c) Brown, C.; Heaton, B. T.; Chini, P.; Fumagalli, A.; Longoni, G. *J. Chem. Soc., Chem. Commun.* **1977**, 309. (d) Washecheck, D. M.; Wucherer, E. J.; Dahl, L. F.; Ceriotti, A.; Longoni, G.; Manassero, M.; Sansoni, M.; Chini, P. *J. Am. Chem. Soc.* **1979**, *101*, 6110. (e) Bengtsson-Kloo, L.; Iapalucci, C. M.; Longoni, G.; Ulvenlund, S. *Inorg. Chem.* **1998**, *37*, 4335.

(5) (a) Roth, J. D.; Lewis, G. J.; Safford, L. K.; Jiang, X.; Dahl, L. F.; Weaver, M. J. *J. Am. Chem. Soc.* **1992**, *114*, 6159. (b) Roth, J. D.; Lewis, G. J.; Jiang, X.; Dahl, L. F.; Weaver, M. J. *J. Phys. Chem.* **1992**, *96*, 7219.

(6) (a) Hwang, G.; Bodenbinder, M.; Willner, H.; Aubke, F. *Inorg. Chem.* **1993**, *32*, 4667. (b) Hwang, G.; Wang, C.; Aubke, F.; Willner, H.; Bodenbinder, M. *Can. J. Chem.* **1993**, *71*, 1532. (c) Hwang, G.; Wang, C.; Bodenbinder, M.; Willner, H.; Aubke, F. *J. Fluorine Chem.* **1994**, *66*, 159.

(7) For detailed reviews, see: (a) Aubke, F.; Wang, C. *Coord. Chem. Rev.* **1994**, *137*, 483. (b) Willner, H.; Aubke, F. *Angew. Chem., Int. Ed. Engl.* **1997**, *36*, 2402.

10.1021/ja000716u CCC: $19.00 
Published on Web 07/08/2000

and are usually prepared in superacids,[8] strong acids such as concentrated $H_2SO_4$,[9] or with weakly coordinating anions.[10] Apart from the CO-bridged dinuclear Pd(I) complex, $[Pd_2(\mu\text{-}CO)_2](SO_3F)_2$,[11] and the unstable dinuclear Hg(I) carbonyl cation, $[Hg_2(CO)_2]^{2+}$,[12] all the complexes are monomeric with values of $\nu$(CO) that are significantly higher than the value of 2143 $cm^{-1}$ for free CO.[13]

A preliminary account of the preparation, together with some spectroscopic data, of the hexacarbonyldiplatinum(I) dication, $[\{Pt(CO)_3\}_2]^{2+}$ (**1**), formed in concentrated sulfuric acid, has recently appeared in a preliminary communication.[14] The discovery of **1** suggests that homoleptic carbonyl cations of the late transition metals in low oxidation states can be formed in media which are less acidic than the superacids that have been previously used and confirms the tendency that carbonyls of metals in lower oxidation states could be formed in media of lower acidity or higher basicity. Despite the unusual Pt(I) oxidation state, **1** shows remarkable stability which presumably arises from the presence of the metal−metal bond. This is the first well-characterized stable, dinuclear, homoleptic, cationic metal carbonyl containing a metal−metal bond unsupported by bridging ligands.

We now report the details of the preparation, characterization by NMR ($^{13}C$ and $^{195}Pt$), IR, Raman and EXAFS spectroscopy, and a density functional calculation for $[\{Pt(CO)_3\}_2]^{2+}$. It is of significant structural interest because **1** represents one of the few simple $M_2L_6$ systems known where M is a transition element.[15−22] Hitherto, the only $M_2(CO)_6$ species known so far is $Cu_2(CO)_6$, which has been prepared in a matrix and shown to possess a "staggered ethane" type structure of approximate $D_{3d}$ symmetry.[20] The geometric optimization for **1** at the B3LYP level predicts that each Pt atom adopts an essentially square-planar geometry; the dihedral angle between the two coordination planes is 90° and the overall symmetry of this complex is $D_{2d}$. **1** is formally isoelectronic with and has a similar structure to the nickel(I) cyanide system $[\{Ni(CN)_3\}_2]^{4-}$,[21] and the isocyanide analogues of Pd(I) and Pt(I), $[\{Pd(CNCH_3)_3\}_2]^{2+}$ and $[\{Pt(CNCH_3)_3\}_2]^{2+}$.[22]

## II. Experimental Section

**(a) Synthesis**. $PtO_2{\cdot}xH_2O$ (Pt, 78.8 wt %; Mitsuwa Pure Chemicals), $H_2SO_4$ (96%, Kanto Chemical Co.), $D_2SO_4$ (96%, CIL), CO (Nippon Sanso), and $^{13}CO$ ($^{13}C$ enrichment 99%, ICON) were used for the preparation of $[\{Pt(CO)_3\}_2]^{2+}$ (**1**) and *cis*-$[Pt(CO)_2]^{2+}{}_{(solv)}$ (**2**).

A mixture of $PtO_2{\cdot}xH_2O$ (2 mmol) and 96% $H_2SO_4$ (10 mL) in a 200-mL three-necked flask was stirred and sonicated (40 kHz, 35 W) for 4 h and the three-necked flask was then evacuated by a rotary pump to remove the air. Carbon monoxide was introduced from a gas balloon so that the flask was kept constantly at 1 atm of CO. The mixture of $PtO_2$ and 96% $H_2SO_4$ was vigorously stirred for 2 weeks at room temperature whereupon the dark colloidal suspension became colorless due to the formation of **1**. The resulting solution is very moisture sensitive. **1** with 99% $^{13}CO$ was similarly prepared using 99% $^{13}CO$ instead of CO. Standard cannula transfer techniques were used for all sample manipulations for the spectroscopic measurements.

The IR spectrum of **1** in 96% $H_2SO_4$ was monitored with time under evacuation (0.001 mmHg). When the band (2174 $cm^{-1}$ for $^{12}CO$ and 2126 $cm^{-1}$ for $^{13}CO$) due to **1** had disappeared (ca. 1 day), nitrogen was admitted to the solution which contained only **2** and a black colloidal precipitate (platinum metal). The pure solution of **2**, which is nearly colorless after precipitation of the colloidal metal, was transferred under nitrogen by cannula and used for all the spectroscopic measurements; this solution is indefinitely stable under a nitrogen atmosphere.

**(b) Instrumentation**. NMR spectra were recorded in $D_2SO_4$ at room temperature using a Bruker AMX 200 with $D_2SO_4$ as a lock. The liquid samples were contained in 10 mm NMR tubes containing a coaxial insert of TMS as the external reference. $^{13}C$ chemical shifts were referenced to external TMS and $^{195}Pt$ chemical shifts were referenced to 42.8 MHz at such a magnetic field that the protons in the external TMS resonate at exactly 200 MHz. NMR simulations were carried out using gNMR 4.1 (Cherwell Scientific, Oxford, UK).

Infrared spectra were obtained at room temperature on thin films between two silicon disks on a JASCO FT/IR-230 spectrometer with a range of 4000−400 $cm^{-1}$ and a spectral resolution of 2 $cm^{-1}$. Raman spectra were recorded at room temperature on a Nicolet FT-Raman 960 spectrometer with a range of 4000−100 $cm^{-1}$ and a spectral resolution of 2 $cm^{-1}$ using the 1064 nm exciting line (~600 mV) of a Nd:YAG laser (Spectra Physics, USA). Liquid Raman samples were contained in a 5-mm o.d. NMR tube.

Platinum $L_{III}$-edge extended X-ray absorption fine structure (EXAFS) spectra were collected in the transmission mode for solutions between two polyethylene films on BL-12C at the Photon Factory of High Energy Accelerator Research Organization (KEK-PF; Tsukuba, Japan), operating at 3 GeV with an average current of 170 mA using a Si-(111) monochromator. Several data sets were collected for each sample in $k$ space ($k$ = photoelectron wave vector/$Å^{-1}$). EXAFS spectra were analyzed according to standard procedures using the REX (Rigaku) program.[23] The preedge region was subtracted with a polynomial function, and then the EXAFS spectrum was extracted by fitting the absorption coefficient with a cubic spline curve and normalized. To

(8) (a) Bach, C.; Willner, H.; Wang, C.; Rettig, S.; Trotter, J.; Aubke, F. *Angew. Chem., Int. Ed. Engl.* **1996**, *35*, 1974. (b) Bröchler, R.; Freidank, D.; Bodenbinder, M.; Sham, I. H. T.; Willner, H.; Rettig, S. J.; Trotter, J.; Aubke, F. *Inorg. Chem.* **1999**, *38*, 3684. (c) Bernhardt, E.; Bley, B.; Wartchow, R.; Willner, H.; Bill, E.; Kuhn, P.; Sham, I. H. T.; Bodenbinder, M.; Bröchler, R.; Aubke, F. *J. Am. Chem. Soc.* **1999**, *121*, 7188.

(9) (a) Xu, Q.; Imamura, Y.; Fujiwara, M.; Souma, Y. *J. Org. Chem.* **1997**, *62*, 1594. (b) Xu, Q.; Souma, Y. *Top. Catal.* **1998**, *6*, 17. (c) Xu, Q.; Souma, Y.; Umezawa, J.; Tanaka, M.; Nakatani, H. *J. Org. Chem.* **1999**, *64*, 6306. (d) Xu, Q.; Nakatani, H.; Souma, Y. *J. Org. Chem.* **2000**, *65*, 1540.

(10) (a) Hurlburt, P. K.; Anderson, O. P.; Strauss, S. H. *J. Am. Chem. Soc.* **1991**, *113*, 6277. (b) Hurlburt, P. K.; Rack, J. J.; Luck, J. S.; Dec, S. F.; Webb, J. D.; Anderson, O. P.; Strauss, S. H. *J. Am. Chem. Soc.* **1994**, *116*, 10003. (c) Polyakov, O. G.; Ivanova, S. M.; Gaudinski, C. M.; Miller, S. M.; Anderson, O. P.; Strauss, S. H. *Organometallics* **1999**, *18*, 3769. (d) Ivanova, S. M.; Ivanov, S. V.; Miller, S. M.; Anderson, O. P.; Solntsev, K. A.; Strauss, S. H. *Inorg. Chem.* **1999**, *38*, 3756.

(11) Wang, C.; Bodenbinder, M.; Willner, H.; Rettig, S.; Trotter, J.; Aubke, F. *Inorg. Chem.* **1994**, *33*, 779.

(12) (a) Willner, H.; Bodenbinder, M.; Wang, C.; Aubke, F. *J. Chem. Soc., Chem. Commun.* **1994**, 1189. (b) Bodenbinder, M.; Balzer-Jöllenbeck, G.; Willner, H.; Batchelor, R. J.; Einstein, F. W. B.; Wang, C.; Aubke, F. *Inorg. Chem.* **1996**, *35*, 82.

(13) Herzberg, G. *Spectra of Diatomic Molecules*, 2nd ed.; van Nostrand: New York, 1950.

(14) Xu, Q.; Souma, Y.; Heaton, B. T.; Jacob, C.; Kanamori, K. *Angew. Chem., Int. Ed. Engl.* **2000**, *39*, 208.

(15) Wilmshurst, J. K. *J. Mol. Spectrosc.* **1960**, *5*, 343.

(16) (a) Harris, C. M.; Livingstone, S. E.; Stephenson, N. C. *J. Chem. Soc.* **1958**, 3697. (b) Stephenson, N. C. *Acta Crystallogr.* **1964**, *17*, 587.

(17) Huq, F.; Mowat, W.; Shortland, A.; Skapski, A. C.; Wilkinson, G. *J. Chem. Soc., Chem. Commun.* **1971**, 1079.

(18) Chisholm, M.; Cotton, F. A.; Frenz, B. A.; Skive, L. *J. Chem. Soc., Chem. Commun.* **1974**, 480.

(19) (a) Willett, R. D.; Dwiggins, C.; Krah, R. F.; Rundle, R. E. *J. Chem. Phys.* **1963**, *38*, 2429. (b) Willett, R. D. *J. Chem. Phys.* **1966**, *44*, 39. (c) Textor, M.; Dubler, E.; Oswald, H. R. *Inorg. Chem.* **1974**, *13*, 1361.

(20) (a) Kündig, E. P.; Moskovits, M.; Ozin, G. A. *Angew. Chem., Int. Ed. Engl.* **1975**, *14*, 292. (b) Huber, H.; Kündig, E. P.; Moskovits, M.; Ozin, G. A. *J. Am. Chem. Soc.* **1975**, *97*, 2097.

(21) (a) Jarchow, O.; Schulz, H.; Nast, R. *Angew. Chem., Int. Ed. Engl.* **1970**, *9*, 71. (b) Jarchow, O. *Z. Anorg. Allg. Chem.* **1971**, *383*, 40. (c) Jarchow, O. *Z. Kristallogr., Kristallgeom., Kristallophys., Kristallchem.* **1972**, *136*, 122.

(22) (a) Doonan, D. J.; Balch, A. L.; Goldberg, S. Z.; Eisenberg, R.; Miller, J. S. *J. Am. Chem. Soc.* **1975**, *97*, 1961. (b) Rettig, M. F.; Kirk, E. A.; Maitlis, P. M. *J. Organomet. Chem.* **1976**, *111*, 113. (c) Goldberg, S. Z.; Eisenberg, R. *Inorg. Chem.* **1976**, *15*, 535. (d) Boehm, J. R.; Doonan, D. J.; Balch, A. L. *J. Am. Chem. Soc.* **1976**, *98*, 4845. (e) Boehm, J. R.; Balch, A. L. *Inorg. Chem.* **1977**, *16*, 778. (f) Lindsay, C. H.; Benner, L. S.; Balch, A. L. *Inorg. Chem.* **1980**, *19*, 3503. (g) Rutherford, N. M.; Olmstead, M. M.; Balch, A. L. *Inorg. Chem.* **1984**, *23*, 2833.

(23) Shen, W.-J.; Ichihashi, Y.; Okumura, M.; Matsumura, Y. *Catal. Lett.* **2000**, *64*, 23.

perform the Fourier transform the EXAFS was multiplied by $k^3$ in the range $k = 3-15$ Å$^{-1}$, and a Hanning window was used. Quantitative analysis was performed by fitting the background-subtracted EXAFS signals using the nonlinear least-squares method and minimization of a $\chi^2$-type function.

**(c) Computational Methods**. The geometry of **1** has been optimized using the empirically parametrized B3LYP exchange-correlation functional in Density Functional Theory (DFT). The present B3LYP functional can be written as

$$F_{(B3LYP)} = (1 - A)Fx_{(Slater)} + AFx_{(HF)} + BFx_{(Becke)} + CFc_{(LYP)} + (1 - C)Fc_{(VWN)} \quad (1)$$

where $Fx_{(Slater)}$ is the Slater exchange, $Fx_{(HF)}$ is the Hartree−Fock exchange, $Fx_{(Becke)}$ is the gradient part of the exchange functional of Becke,[24] $Fc_{(LYP)}$ is the correlation functional of Lee, Yang, and Parr,[25] and $Fc_{(VWN)}$ is the correlation functional of Vosko, Wilk, and Nusair.[26] *A*, *B*, and *C* are the coefficients determined by Becke using the fit to the G1 molecule set. All the calculations were performed with Stevens/Basch/Krauss/Jasien/Cundari-21G (SBK) relativistic effective core potentials (ECP)[27] and their associated basis sets are designed to replace all but the outermost electrons in the Pt atom. The cc-pVTZ[28] general contracted basis sets were applied to the carbon and oxygen atoms in this complex. The vibrational frequencies were computed using B3LYP at the same level of basis sets. The frequency calculations were performed to predict the IR and Raman spectra and identify the nature of the stationary points on the potential energy surfaces. All calculations were carried out using the GAUSSIAN-98 program.[29]

## III. Results and Discussion

**(a) Synthesis**. The first homoleptic Pt(II) carbonyl complex, $[Pt(CO)_4][Pt(SO_3F)_6]$, was isolated by the reductive carbonylation of $Pt(SO_3F)_4$ in $HSO_3F$ with CO at 25 °C according to eq 2:[6a]

$$2Pt(SO_3F)_4 + 5CO \xrightarrow[\sim 2\ atm,\ 25\ ^\circ C]{HSO_3F} [Pt(CO)_4][Pt(SO_3F)_6] + CO_2 + S_2O_5F_2 \quad (2)$$

This reaction represents a partial reduction of Pt(IV) by CO. Increasing the reaction temperature from 25 to 80 °C results in complete reduction to $Pt(CO)_2(SO_3F)_2$, via the yellow intermediate, $[Pt(CO)_4][Pt(SO_3F)_6]$; the overall reaction can be formulated as shown in eq 3:[6c]

$$Pt(SO_3F)_4 + 3CO \xrightarrow[80\ ^\circ C]{HSO_3F} Pt(CO)_2(SO_3F)_2 + CO_2 + S_2O_5F_2 \quad (3)$$

It has been reported that in $SbF_5$, the creamy white complex $Pt(CO)_2(SO_3F)_2$ can be readily converted to the thermally stable, white salt $[Pt(CO)_4][Sb_2F_{11}]_2$ in the presence of a CO atmosphere according to eq 4:[6b]

$$Pt(CO)_2(SO_3F)_2 + 8SbF_5 + 2CO \xrightarrow[60-80\ ^\circ C]{\sim 0.5\ atm\ CO} [Pt(CO)_4][Sb_2F_{11}]_2 + 2Sb_2F_9SO_3F \quad (4)$$

In this study, we find that $[\{Pt(CO)_3\}_2]^{2+}$ (**1**), the first homoleptic, dinuclear platinum(I) carbonyl cation, is formed in concentrated $H_2SO_4$ according to eq 5:

$$2Pt^{IV}O_2 + 9CO + 2H^+ \xrightarrow[room\ temperature,\ 1\ atm]{concentrated\ H_2SO_4} \underset{\mathbf{1}}{[\{Pt^{I}(CO)_3\}_2]^{2+}} + 3CO_2 + H_2O \quad (5)$$

This involves a greater degree of reduction of Pt(IV) than has been observed in superacids[7] and must result from the use of a less acidic medium. The reductive carbonylation of $PtO_2$ by CO takes ca. 2 weeks in concentrated $H_2SO_4$ at room temperature and atmospheric pressure to go to completion and produce a colorless solution of **1**. Prolonged (ca. 1 day) evacuation of the solution of **1** in concentrated $H_2SO_4$ results in disproportionation and the exclusive formation of the nearly colorless complex, *cis*-$Pt(CO)_2^{2+}{}_{(solv)}$ (**2**), according to eq 6:

$$\mathbf{1} \underset{+4CO/concentrated\ H_2SO_4}{\overset{-4CO/concentrated\ H_2SO_4}{\rightleftharpoons}} \underset{\mathbf{2}}{cis\text{-}Pt(CO)_2^{2+}{}_{(solv)}} + Pt^0 \quad (6)$$

This observation indicates that the CO ligands are more weakly bound to Pt(I) in **1** than to Pt(II) in **2**, but more tightly bound than in the Cu(I), Ag(I), Au(I), and Rh(I) carbonyl cations which require only brief evacuation to reversibly remove the CO ligands.[9] Slow reformation of **1** occurs on reintroduction of CO to a solution of **2**. Both **1** and **2** are extremely sensitive to moisture, which results in their immediate decomposition to platinum metal.

**(b) $^{13}$C and $^{195}$Pt NMR Spectroscopy**. The formulation of **1** as a dimer (see Figure 1) results from both the $^{13}$C and $^{195}$Pt NMR studies at natural $^{13}$C abundance and 99% $^{13}$CO enrichment. As shown in Figures 2 and 3, well-resolved spectra are obtained for **1** at ambient temperature, indicating that the structure is rigid on the NMR time scale, whereas the analogous compounds, $(n\text{-}Bu_4N)_2[\{PtX_2(CO)\}_2]$ (X = Cl or Br),[30] and the related Pd(I) isocyanide complex, $[\{Pd(CNCH_3)_3\}_2]^{2+}$,[22e] are both fluxional. By taking into consideration the formulation of **1** which contains three isotopomers, viz., $^{13}C^A(^{13}C^B)_2-{}^{195}Pt-{}^{195}Pt-(^{13}C^B)_2{}^{13}C^A$, $^{13}C^A(^{13}C^B)_2-Pt-{}^{195}Pt-(^{13}C^B)_2{}^{13}C^A$, and $^{13}C^A(^{13}C^B)_2-Pt-Pt-(^{13}C^B)_2{}^{13}C^A$ (for $^{195}$Pt, $I = {}^1/_2$; Pt, $I \neq {}^1/_2$) in the ratio 1:4:4, respectively (see Figure 1 for labeling scheme), the complicated $^{13}$C and $^{195}$Pt NMR spectra of **1** at 99% $^{13}$CO enrichment (Figures 2 and 3) can be well reproduced using the gNMR program with the parameters shown in Table 1.

Previous work has shown that there is *no* correlation of the Pt−Pt bond length, *d*(Pt−Pt), with $^1J$(Pt−Pt′) in closely related dinuclear platinum complexes.[31] It is worthwhile noting that $^1J$(Pt−Pt′) for **1** is 550.9 Hz, which is similar to the value found for the related complex $[\{PtCl(CO)(PPh_3)\}_2]$ (760 Hz)[31] and the analogous isocyanide complex, $[\{Pt(CNCH_3)_3\}_2]^{2+}$ (507 Hz),[31] whereas the value for $^1J$(Pt−Pt′) in $[\{PtCl_2(CO)\}_2]^{2-}$ (5250 Hz)[30] is significantly different, although the other coupling

(24) (a) Becke, A. D. *Phys. Rev. A* **1988**, *38*, 3098. (b) Becke, A. D. *J. Chem. Phys.* **1993**, *98*, 1372. (c) Becke, A. D. *J. Chem. Phys.* **1993**, *98*, 5648.
(25) Lee, C.; Yang, W.; Parr, R. G. *Phys. Rev. B* **1988**, *37*, 785.
(26) Vosko, S. H.; Wilk, L.; Nusair, M. *Can. J. Phys.* **1980**, *58*, 1200.
(27) (a) Stevens, W. J.; Basch, H.; Krauss, M. *J. Chem. Phys.* **1984**, *81*, 6026. (b) Cundari, T. R.; Stevens, W. J. *J. Chem. Phys.* **1993**, *98*, 5555.
(28) Woon, D. E.; Dunning, T. H., Jr. *J. Chem. Phys.* **1993**, *98*, 1358.
(29) Frisch, M. J.; Trucks, G. W.; Schlegel, H. B.; Scuseria, G. E.; Robb, M. A.; Cheeseman, J. R.; Zakrzewski, V. G.; Montgomery, J. A., Jr.; Stratmann, R. E.; Burant, J. C.; Dapprich, S.; Millam, J. M.; Daniels, A. D.; Kudin, K. N.; Strain, M. C.; Farkas, O.; Tomasi, J.; Barone, V.; Cossi, M.; Cammi, R.; Mennucci, B.; Pomelli, C.; Adamo, C.; Clifford, S.; Ochterski, J.; Petersson, G. A.; Ayala, P. Y.; Cui, Q.; Morokuma, K.; Malick, D. K.; Rabuck, A. D.; Raghavachari, K.; Foresman, J. B.; Cioslowski, J.; Ortiz, J. V.; Stefanov, B. B.; Liu, G.; Liashenko, A.; Piskorz, P.; Komaromi, I.; Gomperts, R.; Martin, R. L.; Fox, D. J.; Keith, T.; Al-Laham, M. A.; Peng, C. Y.; Nanayakkara, A.; Gonzalez, C.; Challacombe, M.; Gill, P. M. W.; Johnson, B.; Chen, W.; Wong, M. W.; Andres, J. L.; Gonzalez, C.; Head-Gordon, M.; Replogle, E. S.; Pople, J. A. *Gaussian 98*, Revision A.5; Gaussian, Inc.: Pittsburgh, PA, 1998.
(30) Boag, N. M.; Goggin, P. L.; Goodfellow, R. J.; Herbert, I. R. *J. Chem. Soc., Dalton Trans.* **1983**, 1101.
(31) Boag, N. M.; Browning, J.; Crocker, C.; Goggin, P. L.; Goodfellow, R. J.; Murray, M.; Spencer, J. L. *J. Chem. Res. (M)* **1978**, 2962.

**Table 1.** $^{13}C$ and $^{195}Pt$ NMR Data of $[\{Pt(CO)_3\}_2]^{2+}$ (**1**), *cis*-$Pt(CO)_2^{2+}{}_{(solv)}$ (**2**), and Related Complexes

| compd | $\delta(^{13}C)$ [ppm] | $\delta(^{195}Pt)$ [ppm] | $^1J(Pt-C)$ [Hz] | $^2J(Pt-C)$ [Hz] | $^1J(Pt-Pt')$ [Hz] | ref |
|---|---|---|---|---|---|---|
| $[\{Pt(CO)_3\}_2]^{2+}$(**1**)[a] | 166.3,[b] 158.7[c] | −211.0 | 1281.5,[b] 1595.7[c] | 199.6,[b] −26.2[c] | 550.9[d] | *e* |
| $[\{PtCl_2(CO)\}_2]^{2-}$[f] | 159.2 | 371 | 2000 | 48 | 5250 | 30 |
| $[\{PtBr_2(CO)\}_2]^{2-}$[f] | 159.8 | 192 | 2007 | 48 | 4770 | 30 |
| *cis*-$Pt(CO)_2^{2+}{}_{(solv)}$(**2**)[a] | 133.7 | 957.9 | 1907.3 | | | *e* |
| *cis*-$[Pt(CO)_2(SO_3F)_2]$[g] | 131 | | 2011 | | | 7b |
| *cis*-$[Pt(CO)_2Cl_2]$[h] | 151.6 | | 1576 | | | 38 |
| $[Pt(CO)_4][Sb_2F_{11}]_2$[g] | 137 | | 1550 | | | 7b |

[a] In concentrated $H_2SO_4$. [b] For $^{13}C^A$; see Figure 1 for the labeling scheme. [c] For $^{13}C^B$. [d] Other coupling constants (Hz): $^2J(C^A-C^B) = 0$, $^3J(C^A-C^{A'}) = 19.8$, $^3J(C^B-C^{B'}) = 0$, $^3J(C^A-C^B) = 0$. [e] This paper. [f] In $CD_2Cl_2-CH_2Cl_2$ at ca. 220 K. [g] In the solid state. [h] Spectroscopic data listed were obtained in benzene.

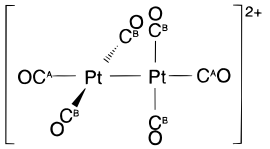


**1**

**Figure 1.** Schematic structure of $[\{Pt(CO)_3\}_2]^{2+}$ (**1**) along with the labeling scheme for the carbonyl groups.


**Figure 2.** $^{13}C$ NMR spectra (50 MHz) of $[\{Pt(CO)_3\}_2]^{2+}$ (**1**) at 99% $^{13}CO$ enrichment in concentrated $D_2SO_4$: (a) observed spectrum and (b) simulated spectrum (gNMR) using the parameters given in Table 1.

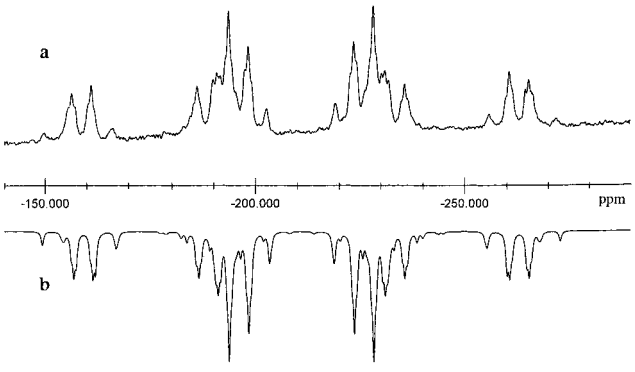


**Figure 3.** $^{195}Pt$ NMR spectra (43 MHz) of **1** at 99% $^{13}CO$ enrichment in concentrated $D_2SO_4$: (a) observed spectrum and (b) simulated spectrum (gNMR) using the parameters given in Table 1.

constants are rather similar (see Table 1 and refs 30 and 31). The coupling constant $^1J(^{13}C-^{195}Pt)$ is larger for the equatorial $C^B$ (1595.7 Hz) than for the axial $C^A$ (1281.5 Hz), and this is consistent with the theoretical calculation that predicts that Pt−$C^B$ is shorter than Pt−$C^A$ (vide infra). For comparison, the coupling constants of $^1J(^{13}C-^{195}Pt)$ are 1550, 2011, 2000, and 2007 Hz for $[Pt(CO)_4][Sb_2F_{11}]_2$,[7b] $Pt(CO)_2(SO_3F)_2$,[7b] $[\{PtCl_2(CO)\}_2]^{2-}$,[30] and $[\{PtBr_2(CO)\}_2]^{2-}$,[30] respectively. The $^{195}Pt$ resonance for **1** (−211.0 ppm) is slightly upfield from the halide derivatives, $[\{PtCl_2(CO)\}_2]^{2-}$ (371 ppm) and $[\{PtBr_2(CO)\}_2]^{2-}$ (192 ppm).[30] The $^{13}C$ chemical shifts for **1** (158.7 and 166.3 ppm) are similar to those found for $[\{PtCl_2(CO)\}_2]^{2-}$ (159.2 ppm) and $[\{PtBr_2(CO)\}_2]^{2-}$ (159.8 ppm),[30] and downfield from the Pt(II) carbonyl complexes, $[Pt(CO)_4][Sb_2F_{11}]_2$ (137 ppm) and $Pt(CO)_2(SO_3F)_2$ (131 ppm);[7b] this is in keeping with the trend that the chemical shift of cationic carbonyl derivatives is observed with smaller values than observed for free $^{13}CO$ (184 ppm), whereas neutral carbonyl complexes and anionic carbonylmetalates have correspondingly higher $\delta$ ($^{13}CO$) values.[7]

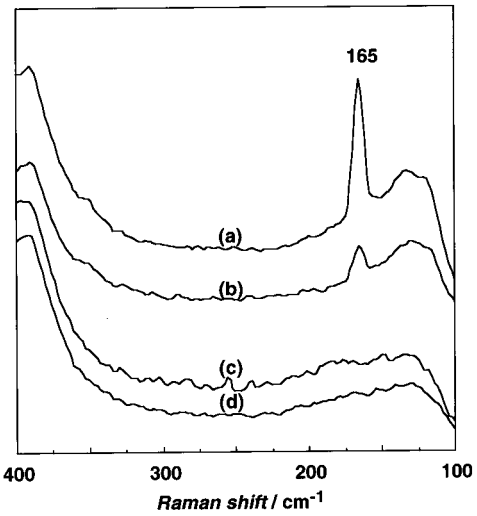


**Figure 4.** Raman spectra (400−100 $cm^{-1}$) of (a) **1** in concentrated $H_2SO_4$ with 0° polarization filter, (b) **1** in concentrated $H_2SO_4$ with 90° polarization filter, (c) concentrated $H_2SO_4$ with 0° polarization filter, and (d) concentrated $H_2SO_4$ with 90° polarization filter.

Prolonged evacuation of **1** results in the disproportionation and formation of **2** through the loss of CO (eq 6). In this case, $^{13}C$ and $^{195}Pt$ NMR measurements on unenriched and 99% $^{13}CO$ enriched **2** show that there are two magnetically equivalent carbonyls per platinum with no Pt−Pt coupling indicating that **2** is a monomer. The $^{195}Pt$ chemical shift for **2** is 957.9 ppm (Table 1), downfield from **1** (−211.0 ppm). The values of $\delta$ ($^{13}CO$) and $^1J(^{13}C-^{195}Pt)$ for **2** are 133.7 ppm and 1907.3 Hz, respectively, which are almost the same as the values found for $Pt(CO)_2(SO_3F)_2$ (131 ppm and 2011 Hz, respectively).[7b]

**(c) Vibrational Spectra**. Figure 4 shows the Raman spectra of **1** in the range of 400−100 $cm^{-1}$. A very strong, sharp band appears at 165 $cm^{-1}$ and is strongly polarized ($\rho$ = ca. 0.25), suggesting a symmetric stretching vibration. Metal−metal bond stretching vibrations characteristically exhibit an intense band in the Raman spectrum[32] and the value observed for **1** is similar to those observed for $(n\text{-}Pr_4N)_2[\{PtX_2(CO)\}_2]$ (X = Cl [170 $cm^{-1}$] and Br [135 $cm^{-1}$])[33] and $[Hg_2(CO)_2][Sb_2F_{11}]_2$ (169

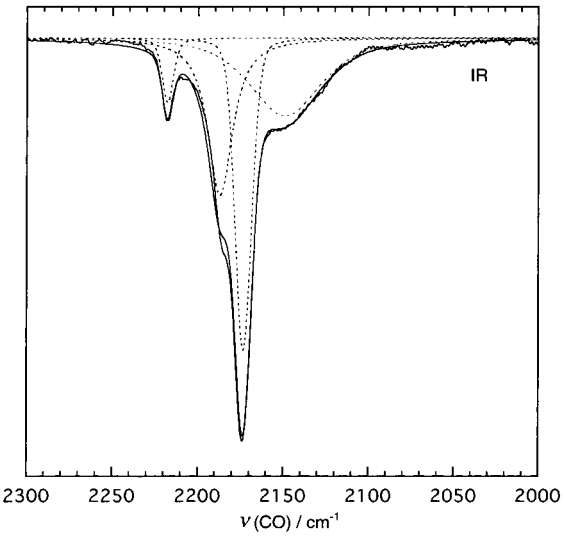


**Figure 5.** IR spectrum of **1** in concentrated $H_2SO_4$. The broad band centered at 2150 $cm^{-1}$ originates from the solvent, concentrated $H_2SO_4$.

$cm^{-1}$).[12] The Raman band at 165 $cm^{-1}$ can be attributed to the Pt−Pt stretching vibration of $A_1$ symmetry, which is also close to the value (151 $cm^{-1}$) predicted by the DFT calculation (vide infra) and confirms that **1** is a dimer with a direct Pt−Pt bond.

For $[\{Pt(CO)_3\}_2]^{2+}$, there are three possible configurations: (a) one involves the two T-shaped $Pt(CO)_3$ groups in the same plane and has $D_{2h}$ symmetry; (b) one has $D_2$ symmetry with the dihedral angle of the two T-shaped $Pt(CO)_3$-coordination planes between 0° and 90.0°; and (c) the other structure has $D_{2d}$ symmetry with a dihedral angle of exactly 90.0°. The group theoretical predictions[34] for the CO stretching modes associated with these geometries are given in eqs 7−9 with the spectroscopic activities shown in parentheses.

$$\Gamma_{CO}^{D_{2h}} = 2A_g\,(R) + B_{1g}\,(R) + B_{2u}\,(IR) + 2B_{3u}\,(IR) \quad (7)$$

$$\Gamma_{CO}^{D_2} = 2A\,(R) + B_1\,(IR, R) + B_2\,(IR, R) + 2B_3\,(IR, R) \quad (8)$$

$$\Gamma_{CO}^{D_{2d}} = 2A_1\,(R) + 2B_2\,(IR, R) + E\,(IR, R) \quad (9)$$

Figures 5 and 6 show the IR and Raman spectra of **1**, respectively, in the CO stretching region. Since the structure with the two T-shaped $Pt(CO)_3$ groups in the same plane is centrosymmetric, there should be no IR/Raman coincidences according to the "mutual exclusion rule",[34] and the structure with $D_{2h}$ symmetry can be ruled out for **1**. Figure 7 shows the normal CO stretching modes predicted by group theory for $[\{Pt(CO)_3\}_2]^{2+}$ with $D_{2d}$ symmetry, which are consistent with those predicted by the DFT calculation at the B3LYP level (vide infra). In Figure 5, the broad IR band centered at 2150 $cm^{-1}$ originates from the solvent, concentrated $H_2SO_4$. The observed IR and Raman bands for **1** shown in Figures 5 and 6 are entirely consistent with the $D_{2d}$ symmetry. The strongly polarized Raman bands at 2233 and 2209 $cm^{-1}$ do not have the corresponding IR counterparts and therefore are assigned to the symmetric CO stretching vibrations ($A_1$). The strongest IR band at 2174 $cm^{-1}$, which has a Raman counterpart with a lower intensity at 2173 $cm^{-1}$, is attributed to the asymmetric $E$ mode. The two depolarized Raman bands at 2194 and 2219 $cm^{-1}$ and the corresponding IR counterparts at 2187 and 2218 $cm^{-1}$ are assigned to the $B_2$ modes.

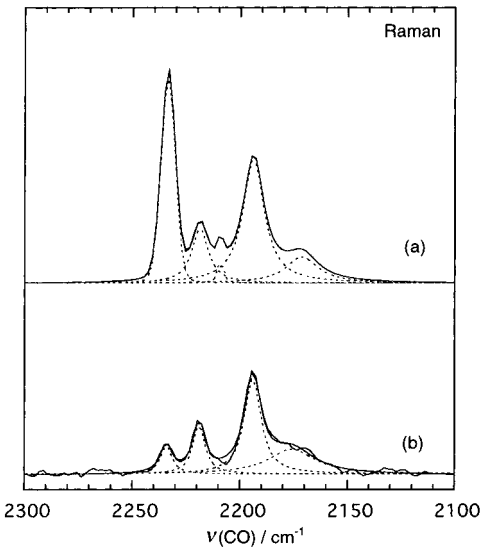


**Figure 6.** Raman spectra of **1** in concentrated $H_2SO_4$: (a) Raman spectrum with 0° polarization filter and (b) Raman spectrum with 90° polarization filter.

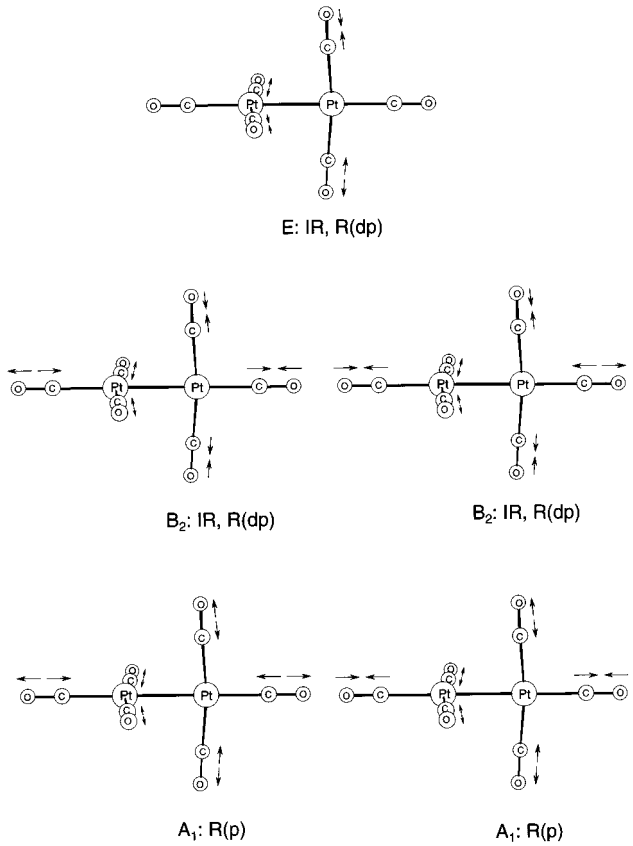


**Figure 7.** Normal CO stretching modes for $[\{Pt(CO)_3\}_2]^{2+}$ (**1**) of $D_{2d}$ symmetry given by the group theoretical predictions and the DFT calculations at the B3LYP level.

The average CO stretching vibrational frequency, $\nu_{av}(CO)$, for **1** is 2199 $cm^{-1}$, higher than 2143 $cm^{-1}$, the value for free CO,[13] but well below the $\nu_{av}(CO)$ of 2261 $cm^{-1}$ for the homoleptic divalent platinum carbonyl cation, $[Pt(CO)_4]^{2+}$;[6b] this is in keeping with a decrease in $\pi$-back-bonding and an increase in $\sigma$-bonding for a homoleptic carbonyl complex of

(32) Spiro, T. *Prog. Inorg. Chem.* **1970**, *11*, 1.
(33) Goggin, P. L.; Goodfellow, R. J. *J. Chem. Soc., Dalton Trans.* **1973**, 2355.
(34) Nakamoto, K. *Infrared and Raman Spectra of Inorganic and Coordination Compounds*, 5th ed.; Wiley-Interscience: New York, 1997.

**Table 2.** Experimental and Calculated (B3LYP/cc-pVTZ) CO Stretching Frequencies of $[\{Pt(CO)_3\}_2]^{2+}$ (**1**), *cis*-$Pt(CO)_2^{2+}{}_{(solv)}$ (**2**), and Related Complexes

| compd | exptl[a] IR | exptl[a] Raman | calcd[a] | sym | ref |
|---|---|---|---|---|---|
| $[\{Pt(CO)_3\}_2]^{2+}$(**1**)[b,c] | 2174 vs | 2173 m, dp[d] | 2186 | *E* | *e* |
| | 2187 sh | 2194 vs, dp | 2206 | $B_2$ | |
| | 2218 s | 2219 s, dp | 2228 | $B_2$ | |
| | | 2209 w, p | 2212 | $A_1$ | |
| | | 2233 vs, p | 2240 | $A_1$ | |
| *cis*-$Pt(CO)_2^{2+}{}_{(solv)}$(**2**)[b,f] | 2182 s | 2182 s, dp | | $B_2$ | *e* |
| | 2218 s | 2219 s, p | | $A_1$ | |
| $(n\text{-}Pr_4N)_2[\{PtCl_2(CO)\}_2]$[g] | 2030, 2046 | 2032, 2044 | | | 33 |
| $(n\text{-}Pr_4N)_2[\{PtBr_2(CO)\}_2]$[g] | 2010, 2028 | 2009, 2027 | | | 33 |
| *cis*-$Pt(CO)_2(SO_3F)_2$[g] | 2185, 2219 | 2181, 2218 | | | 6c |
| *cis*-$[Pt(CO)_2Cl_2]$[h] | 2137, 2178 | 2131, 2172 | | | 38 |
| $[Pt(CO)_4][Sb_2F_{11}]_2$[g] | 2244 | 2267, 2289 | | | 6b |

[a] Wavenumber in $cm^{-1}$; s = strong, m = medium, w = weak, sh = shoulder, v = very, p = polarized, dp = depolarized. [b] In concentrated $H_2SO_4$. [c] The symbols of symmetry species are under $D_{2d}$ symmetry. [d] $\nu(Pt-Pt)_{exptl} = 165\ cm^{-1}$, strongly polarized ($\rho = 0.25$); $\nu(Pt-Pt)_{calcd} = 151\ cm^{-1}$, of $A_1$ symmetry. [e] This work. [f] The symbols of symmetry species are under $C_{2v}$ symmetry. [g] In the solid state. [h] Available as a salt; the spectroscopic data listed here were obtained in bezene solution.

the same metal in the higher oxidation state. $\nu_{av}(CO)$ for **1** is lower than that found for $[Au(CO)_2]^+$ (2235 $cm^{-1}$)[35] and $[Hg_2(CO)_2]^{2+}$ (2248 $cm^{-1}$),[12] but higher than that found for $[Rh(CO)_4]^+$ (2169 $cm^{-1}$).[36,37] On the other hand, replacement of the CO ligands in $[\{Pt(CO)_3\}_2]^{2+}$ by halides causes $\nu_{av}(CO)$ to shift to significantly lower frequencies as seen in $(n\text{-}Pr_4N)_2[\{PtCl_2(CO)\}_2]$ (2038 $cm^{-1}$) and $(n\text{-}Pr_4N)_2[\{PtBr_2(CO)\}_2]$ (2019 $cm^{-1}$).[33] To summarize the discussion on the vibrational spectra of **1** in the CO stretching range, the relevant data have been collected in Table 2 together with the related Pt carbonyl complexes and compared with the predictions by the DFT calculation at the B3LYP level of theory described below.

Figure 8 shows the IR and Raman spectra of the concentrated $H_2SO_4$ solution of **2** which was obtained by evacuation of the solution of **1** for ca. 1 day (eq 6). The broad IR band centered at 2150 $cm^{-1}$ originates from the solvent of concentrated $H_2SO_4$. We presently favor the square-planar Pt(II) which has a cis-conformation and therefore a $C_{2v}$ symmetry; this is consistent with the IR and Raman measurements. The Raman band at 2219 $cm^{-1}$ is strongly polarized, which, along with its IR counterpart at 2218 $cm^{-1}$, is assigned to the symmetric CO stretch ($A_1$). The Raman band at 2182 $cm^{-1}$ is depolarized, which, along with its IR counterpart at 2182 $cm^{-1}$, is assinged to the asymmetric CO stretch ($B_2$). The values of the IR and Raman bands for **2** are higher than those observed for *cis*-$[Pt(CO)_2Cl_2]$,[38] but almost the same as those for *cis*-$Pt(CO)_2(SO_3F)_2$.[6c] It is difficult to be sure whether the other two coordination sites on platinum are occupied by a bidentate $SO_4^{2-}$ or 2 monodentate $SO_4^{2-}/HSO_4^-$ groups since it is impossible to obtain any useful IR or Raman data in the sulfato region. However, in concentrated $H_2SO_4$ solution, it seems more probable that the other two sites are occupied by monodentate $HSO_4^-$ groups as recently found for silver(I).[39]

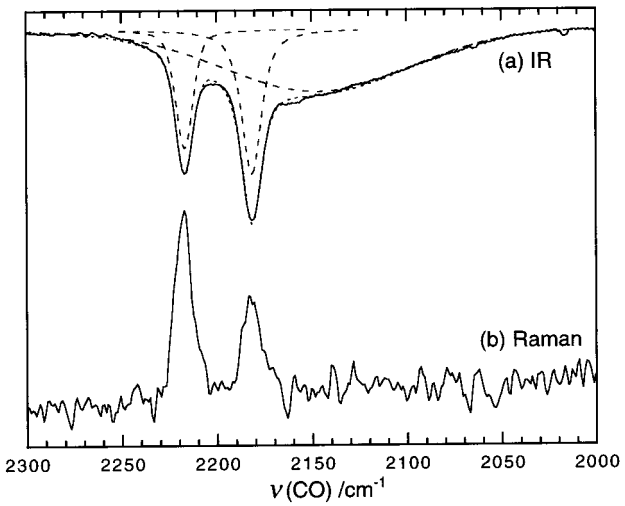


**Figure 8.** IR (a) and Raman (b) spectra of **2** in concentrated $H_2SO_4$. The broad band centered at 2150 $cm^{-1}$ in part a originates from the solvent, concentrated $H_2SO_4$.

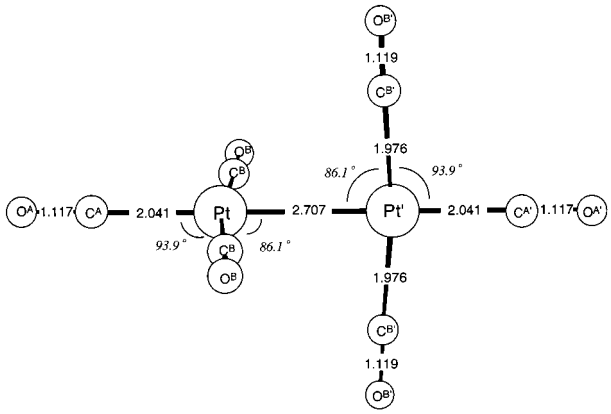


**Figure 9.** Geometry of $[\{Pt(CO)_3\}_2]^{2+}$ (**1**) optimized using B3LYP/cc-pVTZ. The dihedral angle between the two coordination planes of the T-shaped $Pt(CO)_3$ groups is predicted to be exactly 90.0° and the overall symmetry is predicted to be $D_{2d}$. Bond lengths are in Å.

**(d) Density Functional Calculation**. The geometry of $[\{Pt(CO)_3\}_2]^{2+}$ (**1**) has been optimized at the B3LYP level of theory, which is predicted to adopt the overall symmetry of $D_{2d}$ as shown in Figure 9. A direct Pt−Pt bond of 2.707 Å joins the two Pt atoms and each of them adopts an essentially square-planar coordination geometry with the Pt−Pt bond occupying one of the coordination sites. The dihedral angle between the two coordination planes is predicted to be exactly 90.0°. The four "equatorial" $Pt-C^B$ bonds are structurally equivalent. The metal−metal bond shows a large trans influence and thus the "equatorial" $Pt-C^B$ bonds are significantly shorter than the two "axial" $Pt-C^A$ bonds (1.976 vs 2.041 Å). The values are close to the mean length of the Pt−C bonds determined by EXAFS as described below. An additional structural feature is the cis C−Pt−Pt bond angle of 86.1°, indicating displacement of the equatorial CO ligands toward the neighboring Pt atom. Similar distortions have been found for $M_2(CO)_{10}$ (M = Mn, Re), both of which have approximate $D_{4d}$ symmetry and have an average cis C−M−M bond angle of 86.38°.[40] Both of the axial $C^A-O^A$ (1.117 Å) and equatorial $C^B-O^B$ (1.119 Å) bond distances

(35) (a) Willner, H.; Aubke, F. *Inorg. Chem.* **1990**, *29*, 2195. (b) Willner, H.; Schaebs, J.; Hwang, G.; Mistry, F.; Jones, R.; Trotter, J.; Aubke, F. *J. Am. Chem. Soc.* **1992**, *114*, 8972.

(36) (a) Bach, C. Ph.D. Thesis, Hannover, 1999. (b) Lupinetti, A. J.; Havighurst, M. D.; Miller, S. M.; Anderson, O. P.; Strauss, S. H. *J. Am. Chem. Soc.* **1999**, *121*, 11920.

(37) Xu, Q.; Inoue, S.; Souma, Y.; Nakatani, H. *J. Organomet. Chem.* In press.

(38) Browning, J.; Goggin, P. L.; Goodfellow, R. J.; Norton, M. G.; Rattray, A. J. M.; Taylor, B. F.; Mink, J. *J. Chem. Soc., Dalton Trans.* **1977**, 2061.

(39) Dell'Amico, D. B.; Calderazzo, F.; Marchetti, F. *Chem. Mater.* **1998**, *10*, 524.

in **1** are shorter than the bond length of free CO which has been calculated to be 1.126 Å at the same level of calculation (B3LYP/cc-pVTZ) and is in good agreement with the experimental value of 1.128 Å.[41] The observations have the same tendency as observed for the other cationic metal carbonyl complexes.[7]

This structure is related to $[\{PtCl_2(CO)\}_2]^{2-}$ which contains two slightly distorted T-shaped $PtCl_2(CO)$ groups with a dihedral angle of 60° between the two planes and both the CO's on each group are cis to the Pt−Pt bond (2.584 Å).[42] Other related, crystallographically characterized dinuclear platinum carbonyls include $[\{PtCl(CO)(P\text{-}t\text{-}Bu_2Ph)\}_2]$[43] and $[\{Pt(C_6F_5)(CO)(PPh_3)\}_2]$,[44] which have the following dihedral angles, with the Pt−Pt distance (Å) given in parentheses, 70.1° (2.628), and 78.6° (2.599), respectively. Preliminary reports have also appeared for $[\{PtCl(CO)(PPh_3)\}_2]$[31] and, in all cases, the carbonyls are cis and the two phosphines are trans to the Pt−Pt bond. For the crystallographically characterized isocyanide analogue of Pd(I), $[\{Pd(CNCH_3)_3\}_2](PF_6)_2$, the Pd−Pd bond length is 2.531 Å, each Pd atom adopts an essentially square-planar coordination geometry with the Pd−Pd bond occupying one of the coordination sites, and the dihedral angle between the two square planes is 86.2°.[22a] The "axial" Pd−C bonds are significantly longer than the "equatorial" Pd−C bonds, 2.049 vs 1.963 Å, and the cis C−Pd−C bond angles average 95.0°.

The transition state (TS) for **1** has been calculated to contain two bridging CO's and four terminal CO's and have overall $C_{2v}$ symmetry. Its imaginary frequency is 37i $cm^{-1}$ and its imaginary vector belongs to $A_2$ which suggests the intrinsic reaction coordinate (IRC) from the transition state to the $D_{2d}$ minimum. The activation energy for conversion of **1** to this transition state has been calculated to be 31.0 kcal/mol, which is in agreement with **1** being rigid on the NMR time scale at room temperature; this should be contrasted with $[\{Pd(CNCH_3)_3\}_2]^{2+}$ which is fluxional at room temperature and this rearrangement has been suggested to involve a tetrahedral deformation about one metal center, rotation about the Pd−Pd bond, and a return to the square-planar geometry with an activation energy of 13.8 kcal/mol.[22e]

Figure 10 shows the molecular orbitals of **1**. In general, metal carbonyl complexes are described by carbon-to-metal $\sigma$ donation and metal-to-carbon $\pi$ back-donation.[45,46] In this dication complex, there are six orbitals represented by the carbon-to-platinum $\sigma$ donation in $(11b_2)^2(11a_1)^2(12b_2)^2(12a_1)^2(13b_2)^2(13a_1)^2$ [labeled in blue], and six orbitals represented by the platinum-to-carbon $\pi$ back-donation in $(12e)^4(2b_1)^2(2a_2)^2(13e)^4$ [labeled in green]. The molecular orbital coefficient analysis shows that the $\pi$ back-donation is relatively small, and the CO ligands are bound to the Pt center mainly by the $\sigma$ donation. A Mulliken population analysis shows that the gross population is characterized by a $s^{0.72}d^{8.45}$ valence electron configuration on each platinum atom, and the summation of the positive charges on the six CO ligands is +1.53. This means that the charge of the dication complex is relatively localized on the CO ligands as a result of the carbon-to-platinum $\sigma$ donation. The three highest occupied molecular orbitals (HOMO) are represented by the direct Pt−Pt bonding [labeled in red]. Two orbitals of $a_1$ symmetry, $14a_1$ and $15a_1$, can be described as bonding orbitals, and the $14b_2$ orbital as an antibonding orbital between the two Pt atoms. We can find another antibonding orbital between the central Pt atoms in the next LUMO, $15b_2$. The Pt−Pt bonding of this complex can therefore be characterized as a single bond.

The vibrational frequencies for **1** have been computed using the optimized geometry at the B3LYP level of theory. The Raman-active, symmetric Pt−Pt stretch ($A_1$) is predicted to appear at 151 $cm^{-1}$, which is close to the observed Raman band at 165 $cm^{-1}$ (Figure 4). There are five CO stretching modes which are factorized by 0.97 for comparison with the CO stretch of free CO (2143 $cm^{-1}$) at the same B3LYP level. Three CO stretching modes, of which one is the degenerate $E$ mode (2186 $cm^{-1}$) and the other two are the asymmetric $B_2$ modes (2206 and 2228 $cm^{-1}$), are both IR- and Raman-active, and two symmetric $A_1$ modes (2212 and 2240 $cm^{-1}$) are Raman-active but IR-inactive. The vibrational vectors of the CO stretching modes are shown in Figure 7. All the calculated CO stretching frequencies of **1** are higher than that of free CO ($E$, +43 $cm^{-1}$; $B_2$, +63 and +85 $cm^{-1}$; $A_1$, +69 and +97 $cm^{-1}$),[13] as previously observed for other metal carbonyl cations.[7] The calculated CO stretching IR and Raman bands are compared with the experimental results in Table 2.

**(e) Extended X-ray Absorption Fine Structure (EXAFS) Spectroscopy**. Due to our present inability to obtain a single crystal, the bond parameters of **1** have been determined by platinum $L_{III}$-edge EXAFS measurements. The reliability of the data collection and treatment has been confirmed by the collection and analysis of platinum $L_{III}$-edge EXAFS data on $Pt_3(\mu\text{-}CO)_3L_3$ (L = $PPh_2Bz$).[47] The EXAFS results for $Pt_3(\mu\text{-}CO)_3L_3$ (L = $PPh_2Bz$) (Pt−C 2.050 Å, Pt−Pt 2.663 Å, and Pt−P 2.261 Å) are in satisfactory agreement with the data for $Pt_3(\mu\text{-}CO)_3L_3$ (L = $PPh_3$) (averages of Pt−C 2.061 Å, Pt−Pt 2.664 Å, and Pt−P 2.259 Å) from the single-crystal X-ray analysis;[47c] the bond lengths of Pt−C, Pt−Pt, and Pt−P can be considered to be almost the same in both compounds.

For **1** in concentrated $H_2SO_4$ solution, eight data sets were collected and averaged, and the data multiplied by $k^3$ to compensate for the drop-off in intensity at the higher $k$. The fits discussed below are all compared with the averaged raw (background-subtracted) EXAFS data (see Figure 11a). The data were initially modeled to three shells of Pt, C, and O, which were iterated in the usual way, and the best fits tested for statistical significance ($R$ = 13.8%). We found that in the fitting with three shells, the coordination numbers of Pt and C are 1 and 3, respectively, but that of O is 4, which is inconsistent with the structure of **1** that includes three closest O atoms with respect to each Pt atom. Therefore, further modeling of the

(40) (a) Churchill, M. R.; Amoh, K. N.; Wasserman, H. J. *Inorg. Chem.* **1981**, *20*, 1609. (b) Martin, M.; Rees, B.; Mitschler, A. *Acta Crystallogr.* **1982**, *B38*, 6.

(41) Huber, H.; Herzberg, G. *Constants of Diatomic Molecules*; van Nostrand: New York, 1979.

(42) Modinos, A.; Woodward, P. *J. Chem. Soc., Dalton Trans.* **1975**, 1516.

(43) Couture, C.; Farrar, D. H.; Fisher, D. S.; Gukathasan, R. R. *Organometallics* **1987**, *6*, 532.

(44) Usón, R.; Forniés, J.; Espinet, P.; Fortuño, C.; Tomás, M.; Welch, A. J. *J. Chem. Soc., Dalton Trans.* **1989**, 1583.

(45) (a) Hall, M. B.; Fenske, R. F. *Inorg. Chem.* **1972**, *11*, 1620. (b) Sherwood, D. E.; Hall, M. B. *Inorg. Chem.* **1980**, *19*, 1805. (c) Williamson, R. L.; Hall, M. B. *Int. J. Quantum Chem.* **1987**, *21S*, 503. (d) Pierfoot, K.; Verhulst, J.; Verbeke, P.; Vanquickenborne, L. G. *Inorg. Chem.* **1989**, *28*, 3059. (e) Smith, S.; Hillier, I. H.; von Niessen, W.; Guest, M. F. *Chem. Phys.* **1987**, *135*, 357. (f) Barnes, L. A.; Rosi, M.; Bauschlicher, C. W. *J. Chem. Phys.* **1991**, *94*, 2031. (g) Blomberg, M. R. A.; Siegbahn, P. E. M.; Lee, T. L.; Rendell, A. P.; Rice, J. E. *J. Chem. Phys.* **1991**, *95*, 5898. (h) Yamamoto, S.; Kashiwagi, H. *Chem. Phys. Lett.* **1993**, *205*, 306.

(46) For alternative views of the nature of the transition metal−carbonyl bond, see: (a) Hirai, K.; Kosugi, N. *Can. J. Chem.* **1992**, *70*, 301. (b) Davidson, E. R.; Kunze, K. L.; Machado, B. C.; Chakravorty, S. J. *Acc. Chem. Res.* **1993**, *26*, 628.

(47) (a) Chatt, J.; Chini, P. *J. Chem. Soc. (A)* **1970**, 1538. (b) Albinati, A. *Inorg. Chim. Acta* **1977**, *22*, L31. (c) Jiang, A.; Cong, Q. *J. Struct. Chem.* **1985**, *4*, 96.

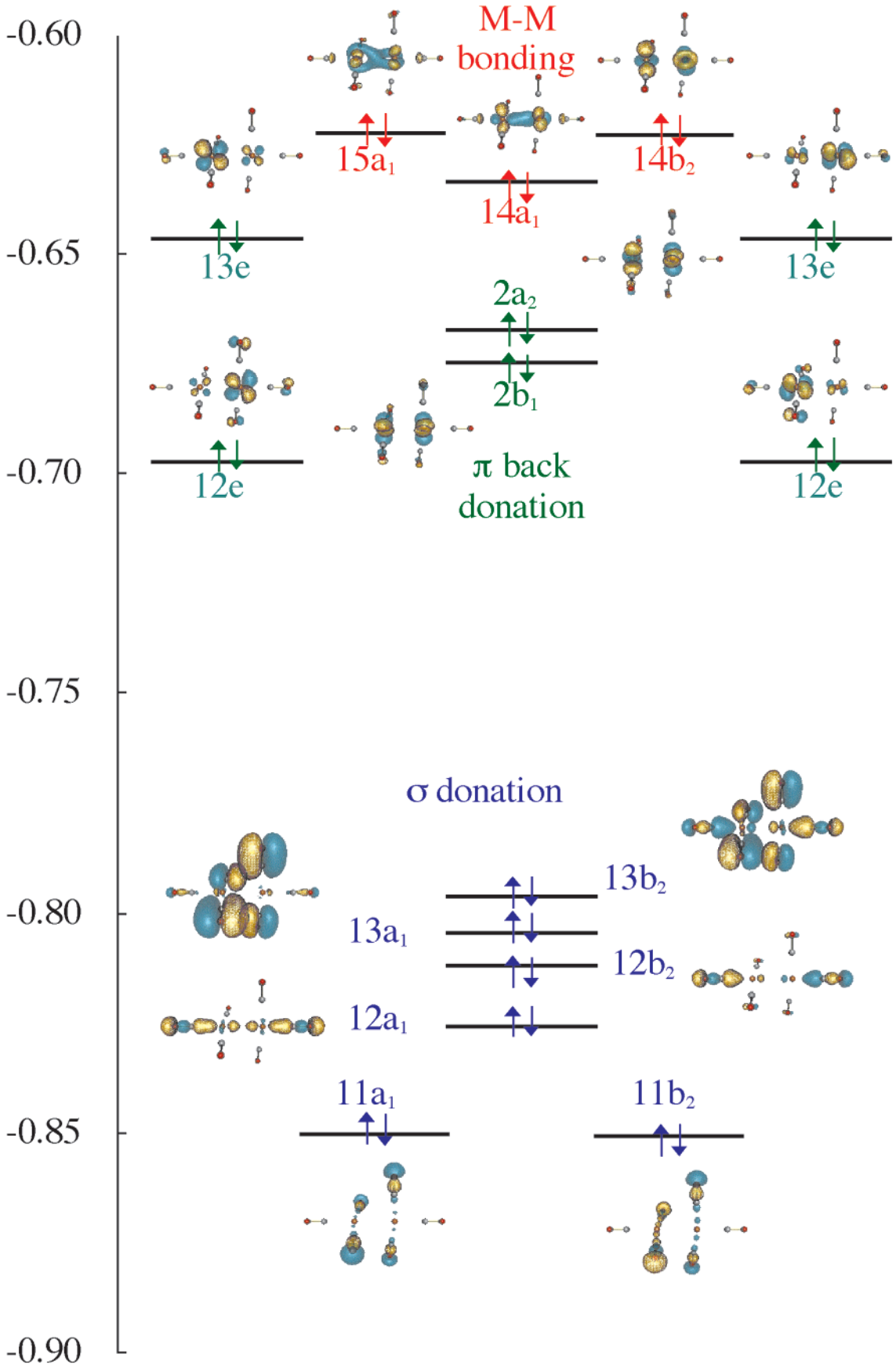


**Figure 10.** Molecular orbital energy diagram of $[\{Pt(CO)_3\}_2]^{2+}$ (**1**) calculated using B3LYP/cc-pVTZ.

EXAFS data was attempted using a four-shell model, the extra shell $C^{B'}$ being the two C atoms coordinated to the neighboring Pt′ atom, which were iterated in the usual way, and the best fits tested for statistical significance (see Table 3). A significant decrease in the *R* factor (to 7.96%) resulted, while the Pt−C and Pt−Pt bond distances were invariant within the normal

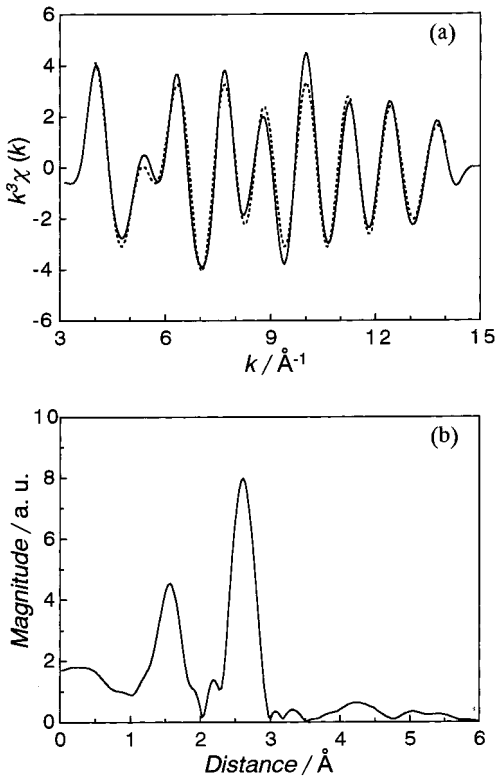


**Figure 11.** Background-subtracted EXAFS (a) (solid line, experimental $\times k^3$; dotted line, curved-wave theory $\times k^3$) and the Fourier transform spectrum (b) for **1** in concentrated $H_2SO_4$; $k$ is the photoelectron wave vector.

**Table 3.** Platinum $L_{III}$-edge EXAFS Data[a] for **1** in Concentrated $H_2SO_4$

| shell | $N$[b] | $d$(EXAFS) [Å] | $\sigma$[c] [Å] |
|---|---|---|---|
| Pt−C[d] | 2.88 | 1.960 | 0.10 |
| Pt−Pt | 0.84 | 2.718 | 0.05 |
| Pt···O[e] | 3.48 | 3.093 | 0.01 |
| Pt···C$^{B'}$[f] | 1.90 | 3.227 | 0.02 |

[a] $R = [\int(\chi^T - \chi^E)k^3\,dk/\int\chi^E k^3\,dk] = 7.96\%$. [b] Coordination number. [c] Debye−Waller factor. [d] Mean length of the Pt−C$^A$ and Pt−C$^B$ bonds. [e] Mean distance of the Pt···O$^A$ and Pt···O$^B$ bonds. [f] Distance between the Pt atom and the equatorial C$^{B'}$ atom coordinated to the neighboring Pt′ atom with which the cis C−Pt−Pt bond angle is calculated to be approximately 85.6°.

precision (±0.01 Å), giving the mean lengths of the Pt−Pt and Pt−C bonds of 2.718 and 1.960 Å, respectively. The Pt−Pt distance of 2.718 Å for **1** is longer than that found for $[\{PtCl_2(CO)\}_2]^{2-}$ (2.584 Å),[42] $[\{PtCl(CO)(P\text{-}t\text{-}Bu_2Ph)\}_2]$ (2.628 Å),[43] and $[\{Pt(C_6F_5)(CO)(PPh_3)\}_2]$ (2.599 Å),[44] but shorter than that found for Pt metal (2.774 Å).[48] The mean Pt−C distance of 1.960 Å is longer than that found for *cis*-$Pt(CO)_2(SO_3F)_2$ (1.854 Å);[7b] this is consistent with the observation that the CO ligands are more weakly bound to Pt(I) in **1** than to Pt(II) in **2** since evacuation of **1** results in the formation of **2** through loss of CO. From the mean lengths of Pt−Pt, Pt−C, and Pt−C′, the cis C−Pt−Pt bond angle is calculated to be approximately 85.6°, indicating displacement of the equatorial CO ligands toward the neighboring Pt atom as predicted by the geometric optimization using B3LYP.

In summary, the bond parameters in **1** have been determined by EXAFS measurements, which confirms the existence of a direct Pt−Pt bond and satisfactorily agrees with the theoretical results at the B3LYP level (Figure 9).

(48) Hartley, F. R. *The Chemistry of Platinum and Palladium*; Applied Science Publishers: London, 1973.

## IV. Conclusions and Summary

The reductive carbonylation of $PtO_2$ allows the facile generation of hexacarbonyldiplatinum(I), $[\{Pt(CO)_3\}_2]^{2+}$, in concentrated sulfuric acid. This reaction indicates that homoleptic carbonyl cations of the late transition metals in low oxidation states can be formed in media which are less acidic than the superacids that have been previously used. Prolonged evacuation of the concentrated $H_2SO_4$ solution of $[\{Pt(CO)_3\}_2]^{2+}$ results in disproportionation and the exclusive formation of the *cis*-$Pt(CO)_2^{2+}{}_{(solv)}$ complex.

The new complex, $[\{Pt(CO)_3\}_2]^{2+}$, is the first well-characterized stable, homoleptic metal carbonyl cation containing a metal−metal bond unsupported by bridging ligands. Its formulation containing two T-shaped $Pt(CO)_3$ groups results from both $^{13}C$ and $^{195}Pt$ NMR studies at natural $^{13}C$ abundance and 99% $^{13}CO$ enrichment. At room temperature its structure is rigid on the NMR time scale in contrast with the nonrigidity of its isocyanide analogue, $[\{Pt(CNCH_3)_3\}_2]^{2+}$. The value of $^1J$(Pt−Pt′) for $[\{Pt(CO)_3\}_2]^{2+}$ is 550.9 Hz, almost the same as that for $[\{Pt(CNCH_3)_3\}_2]^{2+}$ (507 Hz). A strongly polarized, sharp Raman band due to the symmetric Pt−Pt stretch has been observed at 165 $cm^{-1}$. IR and Raman spectra in the CO stretching region are entirely consistent with the presence of only terminal CO's on a nonbridged Pt−Pt bond with a $D_{2d}$ symmetry. The average CO stretching frequency, $\nu_{av}$(CO), is 2199 $cm^{-1}$, higher than 2143 $cm^{-1}$, the value for free CO, but well below the $\nu_{av}$(CO) of 2261 $cm^{-1}$ for the homoleptic divalent platinum carbonyl cation, $[Pt(CO)_4]^{2+}$.

The complex, $[\{Pt(CO)_3\}_2]^{2+}$, represents one of the few simple $M_2L_6$ systems known where M is a transition element. Its geometric optimization at the B3LYP level predicts that each Pt atom possesses an essentially square-planar coordination geometry, the dihedral angle between the two coordination planes is 90°, and the overall complex symmetry is $D_{2d}$. The cis C−Pt−Pt bond angle is 86.1°, indicating displacement of the equatorial CO ligands toward the neighboring Pt atom. This structure is similar to that of the nickel(I) cyanide system $[\{Ni(CN)_3\}_2]^{4-}$ and the isocyanide analogues of Pd(I) and Pt(I), $[\{Pd(CNCH_3)_3\}_2]^{2+}$ and $[\{Pt(CNCH_3)_3\}_2]^{2+}$. $[\{Pt(CO)_3\}_2]^{2+}$ is the first metal carbonyl complex with the $[\{Ni(CN)_3\}_2]^{4-}$-like structure. The metal−metal bond in $[\{Pt(CO)_3\}_2]^{2+}$ shows a large trans influence and thus the "equatorial" Pt−C bonds are significantly shorter than the "axial" Pt−C bonds (1.976 vs 2.041 Å), as observed for its isocyanide analogues of Pd(I), $[\{Pd(CNCH_3)_3\}_2]^{2+}$ (1.963 vs 2.049 Å). EXAFS measurements give bond parameters in satisfactory agreement with the theoretical results.

The new dinuclear Pt(I) carbonyl, $[\{Pt(CO)_3\}_2]^{2+}$, enhances the increasing class of homoleptic metal carbonyl cations; its unusual structure enriches the understanding of cluster chemistry containing direct metal−metal bonding.[49] It has been found that $[\{Pt(CO)_3\}_2]^{2+}$ exhibits high catalytic activity for the carbonylation of olefins.[9b] Future studies will investigate the detailed reaction mechanism of this catalytic activity and attempts will be made to obtain the new complex as a crystalline salt.

**Acknowledgment.** Dr. H. Kageyama, Prof. L. Bengtsson-Kloo, and Dr. J. A. Iggo are acknowledged for their valuable discussions and EPSRC for financial support.

JA000716U

(49) (a) Shriver, D. F.; Kaesz, H. D.; Adams, R. D., Eds. *The Chemistry of Metal Cluster Complexes*; VCH: New York, 1990. (b) Braunstein, P., Oro, L. A., Raithby, P. R., Eds. *Metal Clusters in Chemistry*; Wiley-VCH: Weinheim, 1999.